Van-Thuyet Ngo

INFLUENCE OF VERTICAL LOAD ON PERFORMANCE OF A PROTOTYPE UN-BONDED FIBER REINFORCED ELASTOMERIC ISOLATOR

UTICAJ VERTIKALNOG OPTEREĆENJA NA PERFORMANSE PROTOTIPA IZOLATORA OD ELASTOMERA OJAČANOG NEVEZANIM VLAKNIMA

Originalni naučni rad / Original scientific paper
UDK /UDC:

Rad primljen / Paper received: 12.01.2021

Adresa autora / Author's address:
Faculty of Civil Engineering, Thuyloi University, 175 Tay Son, Dong Da, Hanoi, Vietnam
email: thuyet.kcct@tlu.edu.vn

Keywords
- base isolation
- un-bonded fiber reinforced elastomeric isolator
- rollover deformation
- vertical load
- horizontal behaviour

Abstract

Un-bonded fiber reinforced elastomeric isolator (U-FREI) is an improved device for mitigation of the seismic response of low-rise buildings. It is installed directly between substructure and superstructure without any connection at the interfaces. The horizontal load-displacement behaviour of an U-FREI subjected to the simultaneous action of vertical load and cyclic horizontal displacement is nonlinear due to rollover deformation and the horizontal stiffness of the isolator is a function of both vertical load and horizontal displacement. Most existing studies concerning the influence of vertical load on horizontal behaviour of isolators are carried out for scaled models of conventional bonded isolators. In this paper, horizontal behaviour of a prototype U-FREI is investigated under the action of varying vertical loads and cyclic horizontal displacements by finite element (FE) analysis and then the influence of vertical load on the performance of the isolator is evaluated. FE analysis results indicate that the effective horizontal stiffness of the U-FREI decreases with the increase in vertical load at a given amplitude of horizontal displacement.

Ključne reči
- izolacija temelja
- elastomerni izolator ojačan nevezanim vlaknima
- deformacija valjanjem
- vertikalno opterećenje
- horizontalno ponašanje

Izvod

Elastomerni izolator ojačan nevezanim vlaknima (U-FREI) predstavlja unapređen sistem za ublažavanje seizmičkog odziva kod nižih zgrada. Instalira se direktno između podstrukture i superstrukture bez elemenata veze. Ponašanje opterećenja-pomeranja u horizontalnom pravcu kod U-FREI koji je pod istovremenim dejstvom vertikalnog opterećenja i cikličnog horizontalnog pomeranja, je nelinearno usled deformacija valjanja, a horizontalna krutost izolatora je funkcija vertikalnog opterećenja i horizontalnog pomeranja. Većina istraživanja koja se bave uticajem vertikalnog opterećenja na horizontalno ponašanje izolatora se izvode na modelima u razmeri sa konvencionalnim izolatorima sa vezanim vlaknima. U radu je istraženo horizontalno ponašanje prototipa U-FREI pod dejstvom promenljivih vertikalnih opterećenja i cikličnih horizontalnih pomeranja primenom analize konačnim elementima (FE), a zatim i uticaj vertikalnog opterećenja na performanse izolatora. Rezultati analize FE pokazuju da se efektivna horizontalna krutost U-FREI smanjuje sa povećanjem vertikalnog opterećenja zadate amplitude horizontalnog pomeranja.

INTRODUCTION

Base isolation is an efficient and viable method to reduce the vulnerability of a structure in high seismic risk zones. Transmission of earthquake energy to the structures can be reduced by increasing the fundamental eigenperiod of structures for horizontal motion. In general, base isolators are installed in between the substructure and superstructure to achieve a desired horizontal eigenperiod of the structure.

The idea of base isolation technology for seismic protection of buildings was conceptualized during the early part of twentieth century; however it has been used as one of the most effective anti-seismic equipment only during the last four decades. The main goal of the base isolation is decoupling the superstructure from the substructure resting on shaking ground and protecting the substructure as the vulnerable component of a bridge or a building. Increasing the fundamental period of the structure is the most important mechanism of the seismic isolation system in buildings or bridges that minimizes the internal state of stress, which depends on the characteristics of the dynamic behaviour of the system. Vasiliadis /1/ studied the effect of isolation system period on the seismic response of low-rise retrofitted reinforced concrete building in Greece. The eigenvalue modal analyses of quasi-isolated highway bridges with seat-type abutments were performed to reveal modal response characteristics of the bridges, /2/. Kumar and Petwal /3/ presented the reduction of acceleration response of base-isolated three-storey building with lead plug bearings constructed at Indian Institute of Technology Guwahati, India, as compared to that of fixed-base building.

The above-mentioned studies were carried out on base-isolated structures with steel-reinforced elastomeric isolator (SREI). Conventionally, a SREI consists of elastomer/rubber layers interleaved with steel shims as reinforcement and two steel end plates at top and bottom. In general, SREIs are heavy and relatively expensive. Thus, they are often applied

for large, important buildings like hospitals and emergency centres in developed countries but not so widely used for ordinary low-rise buildings. Fiber reinforced elastomeric isolator (FREI) can possibly be an alternative to SREI in an effort to reduce the weight, cost, and for enabling easy installation.

In view of the above, Kelly /4/ proposed a new light-weight isolator by replacing the steel shims with fiber-reinforced polymer materials. Fiber layers can be produced from carbon or glass. Fiber allows a simpler, less labour-intensive manufacturing process, which would reduce fabrication cost. Therefore, FREIs are likely to provide low cost solutions for seismic isolation of low-rise buildings. Studies on un-bonded fiber reinforced elastomeric isolator (U-FREI) are a significant step towards understanding their response, which will enable their efficient design as seismic isolators in buildings. Generally, U-FREIs have elastomer layers at their bottom and top surfaces, which develop frictional contact with the substructure and superstructure respectively without any special connection for this purpose. This not only makes U-FREIs lighter and less expensive, since steel end plates are not needed for their construction, but also makes their installation process easier. As a result, the implementation of U-FREIs for seismic response control of low-rise lifeline buildings in developing countries is more affordable, compared to SREIs.

Recently, a number of studies have been conducted for obtaining the mechanical characteristics of FREIs, leading to better understanding of their behaviour /5-14/. In most of the previous studies, the horizontal behaviour of FREIs was carried out under a constant vertical load (or a constant vertical pressure) and cyclic horizontal displacement. However, for a base isolation system, an isolator may be subjected to varying values of vertical load and these values may be different from the initial design value. For example, the vertical load on an isolator in a bridge structure is dependent on traffic volume. When the traffic congestion occurs, the bridge decks are subjected to higher loads and thus the value of vertical load on the isolator also becomes higher than the value of the design vertical load. On the contrary, when the traffic volume is sparse, this value of vertical load on the isolator will be lower. Another example is that, for a base isolated building, the vertical loads on isolators correspond to factored column loads and these values may be different for different columns of the building. Thus, it is necessary to study the influence of vertical load on the horizontal behaviour of an isolator.

There are few studies in the literature concerning the effect of vertical load on the horizontal behaviour of isolators. Studies were carried out to analyse the stability of elastomeric isolators and model their behaviour; then the effect of vertical load on the horizontal stiffness of isolators was evaluated, /15-17/. As can be seen, most existing studies concerning the influence of vertical load on performance of isolators were carried out for conventional bonded SREIs. However, the horizontal behaviour of U-FREI is relatively different in comparison with that of conventional bonded isolator. When an isolator is horizontally displaced, the upper and lower faces of conventional isolator remain fully in contact with the support surfaces, while the upper and lower faces of U-FREI roll off the contact surfaces. The reduction of horizontal stiffness of U-FREI with increasing horizontal displacement is dependent on the contact area of the isolator with support surfaces or rollover deformation. Furthermore, there are few studies concerning the effect of vertical load on the horizontal behaviour of an U-FREI, e.g. De Raaf et al. /18/ presented experimentally the horizontal response of a scaled model of U-FREI under the variation of vertical loads and cyclic horizontal displacements to predict the stability of the isolator. Thus, the influence of vertical load on the horizontal behaviour of a prototype U-FREI should be further studied.

From the review of the literature, it has been observed that most of the experimental and numerical studies were carried out on scaled models of FREIs with relatively low shape factors (less than 10). The shape factor (S) is defined as the ratio of the loaded area to load-free area of an elastomer layer /19/. There is little information for isolators with shape factors typical for seismic isolation in the range 10 to 20. Thus, the horizontal behaviour of a prototype U-FREI under the variation of vertical load and cyclic horizontal displacement is required to evaluate the influence of vertical load on its behaviour.

This study investigates the horizontal behaviour of a prototype U-FREIs under the action of varying vertical loads and cyclic horizontal displacements by finite element (FE) analysis. A prototype U-FREI with size of 250×250×100 mm and shape factor of 12.5 is investigated to determine the influence of the vertical load on its mechanical properties including effective horizontal stiffness and equivalent viscous damping factor.

DETAILS OF PROTOTYPE U-FREI

The prototype U-FREIs considered in this study are designed for seismic isolation of a two-storey masonry building under-construction at Tawang, India /11, 20/. These isolators are manufactured by vulcanizing elastomer layers and bi-directional (0°/90°) carbon fiber fabric with the support of METCO Pvt. Ltd., Kolkata, India. Figure 1 shows the view of a typical isolator with component layers and specimens of the U-FREI. The isolator comprises of eighteen elastomer layers interleaved and bonded with seventeen layers of carbon fiber reinforcement sheets. The thickness of each elastomer layer is t_e = 5 mm, while that of each fiber layer is t_f = 0.55 mm. The total height of elastomer is t_r = 90 mm and the total height of the isolator is h = 100 mm. The plan dimensions of the isolator are 250×250 mm. Shape factor of the isolator is S = 12.5 which is substantially higher than that of model U-FREIs used in most of the previous investigations. The shear modulus, G, of the elastomer is 0.90 MPa and the elastic modulus of carbon fiber laminate, E, is 40 GPa.

(a)

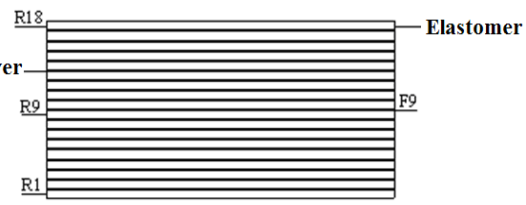

(b)

Figure 1. Details of prototype U-FREI: a) elastomer and fiber layers in the prototype U-FREI; b) specimens.

FE MODELLING

U-FREI exhibits high geometrical nonlinearity under the action of large imposed horizontal displacement and horizontal stiffness thus varies nonlinearly with isolator horizontal deformation. No closed form acceptable analytical solutions are available for estimating the horizontal stiffness of this type of complex un-bonded FREI. In this paper, U-FREI is numerically simulated using ANSYS v.14.0 /21/, a general purpose finite-element software. The isolator is subjected to a variation of the vertical load and cyclic horizontal displacement to evaluate the influence of vertical load on the performance of the isolator in an un-bonded application. FE analysis can address many issues which are rather difficult to be taken into account in closed-form solutions. Furthermore, FE analysis can easily evaluate the response of the prototype isolator under high vertical load and large horizontal displacement, which is very difficult experimentally due to capacity limitations of the experimental facility.

FE modelling of U-FREI is a challenging task as it involves large strain, incompressibility of the material and nonlinear solution convergence. Incompressible material behaviour may lead to some difficulties in numerical simulation, such as volumetric locking, inaccuracy of solution, checkerboard pattern of stress distributions, or occasionally, divergence. A three-term Ogden model is considered to represent the behaviour of elastomer as hyper-elastic material. The type of finite element used for the discretization of the elastomer is selected so that it simulates material behaviour with high incompressibility. Lagrange multiplier-based mixed *u-P* elements are used to simulate the deformation of fully incompressible hyper-elastic materials. Lagrange multipliers extend the internal virtual work so that the volume constraint is included explicitly. The FE analyses have been carried out for multiple cases and no serious convergence issues are encountered.

Element type for FE model

The elastomer exhibits nonlinear behaviour under large displacement. It is modelled using SOLID185, which is an eight-node structural solid element having three degrees of freedom at each node: translations in the nodal *x*, *y*, and *z* directions. This element has the capabilities to model plasticity, hyper-elasticity, stress stiffening, creep, large deflection and large strain behaviour of material. It also has Lagrange multiplier-based mixed *u-P* formulation capability for simulating deformations of nearly incompressible elasto-plastic materials, and fully incompressible hyper-elastic materials. The fiber reinforcement layers are modelled using SOLID46, which is a 3-D eight-node layered structural solid designed to model layered thick shells or solid. Fiber-reinforcements are provided in the form of bi-directional (0°/90°) layers alternated and bonded between elastomer layers. Arrangement of fiber layers (0°/90°) used as reinforcement in isolators is shown in Fig. 2. This element allows up to 250 different material layers. Two rigid horizontal plates are considered at the top and bottom of the isolator to represent the superstructure and substructure. These plates are also modelled using SOLID185.

In order to study U-FREI, the surface-to-surface contact elements are used. Contact elements CONTA173 are used to define the uppermost and undermost elastomer surfaces and target elements TARGE170 are used to define the interior surfaces of top and bottom rigid plates. The contact element supports the Coulomb friction model to transfer the shear forces at the interface of contact and target surface. The coefficient of friction at the contact surfaces of the isolator and the rigid supports is selected to be 0.85, /20/.

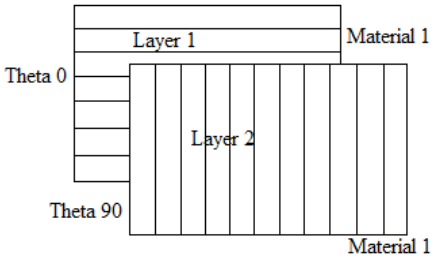

Figure 2. Layer stacking of the fiber-reinforcement in the isolator.

Boundary conditions: the vertical load and horizontal displacement are applied at the top plate, which is allowed to move both in the vertical and horizontal directions, while all degrees of freedom of bottom plate are restrained.

Material model

The elastomer is modelled with hyper-elastic and visco-elastic parameters. Hyper-elasticity refers to materials which can experience large elastic strain that is recoverable. Rubber-like and many other polymer materials fall in the category. The constitutive behaviours of hyper-elastic materials are usually derived from the strain energy potentials. Further, hyper-elastic materials generally have very small compressibility. Finally, hyper-elastic materials have a stiffness that varies with the stress level.

The Ogden three-term model has been adopted to model the hyper-elastic behaviour of the elastomer, which is characterized by shear (G_e) and bulk (K_e) modulus of the elastomer and the visco-elastic behaviour is modelled by Prony Visco-elastic Shear Response parameters.

For the Ogden hyper-elastic material constant:

This option, TB,HYPER,,,,OGDE uses the Ogden form of strain energy potential. The Ogden form is based on the principal stretches of the left Cauchy-Green tensor. The strain energy potential is /21/:

$$W = \sum_{i=1}^{N} \frac{\mu_i}{\alpha_i}(\bar{\lambda}_1^{\alpha_i} + \bar{\lambda}_2^{\alpha_i} + \bar{\lambda}_3^{\alpha_i} - 3) + \sum_{k=1}^{N} \frac{1}{d_k}(J-1)^{2k} . \quad (1)$$

where: W - strain energy potential; $\bar{\lambda}_p$ $(p = 1,2,3)$ = deviatoric principal stretches, defined as $\bar{\lambda}_p = J^{-\frac{1}{3}}\lambda_p$; λ_p - principal stretches of the left Cauchy-Green tensor; J - determinant of the elastic deformation gradient F; N - number of terms in the model; μ_p - shear moduli at the reference configuration; α_p - dimensionless material constants; N, μ_p, α_p and d_p - material constants.

The initial shear modulus μ_0 is defined by:

$$\mu_0 = \frac{1}{2}\sum_{p=1}^{N} \alpha_p \mu_p . \quad (2)$$

According to /22-23/, the Odgen three-term model of elastomer material is given by:

$N = 3$;

$\mu_1 = 6.30\times10^5$ N/m^2; $\alpha_1 = 1.3$;

$\mu_2 = 0.012\times10^5$ N/m^2; $\alpha_2 = 5.0$;

$\mu_3 = -0.10\times10^5$ N/m^2; $\alpha_3 = -2.0$.

The initial bulk modulus (K) is defined by:

$$K = \frac{2}{d} . \quad (3)$$

The shear modulus (G_e) and the bulk modulus (K_e) of the elastomer can be computed by

$$G_e = \frac{E}{2(1+\mu_e)} . \quad (4)$$

$$K_e = \frac{E}{3(1-2\mu_e)} . \quad (5)$$

where: E is Young's modulus; and μ_e is Poisson's ratio of the elastomer material. According to /24/, the Poisson's ratio of the elastomer material is approximately 0.4998.

For the Prony Viscoelastic Shear Response parameters:

Use the TB,PRONY,,,,SHEAR commands to input the relaxation property. The data representing a time-dependent or viscoelastic response of materials can be approximated by a Prony series, based on a relaxation or creep test. For elastomer material of FREIs, the Prony Shear Response parameters are $\alpha_1 = 0.3333$; $t_1 = 0.04$; $\alpha_2 = 0.3333$; $t_2 = 100$.

Details of input loads

Horizontal behaviour of U-FREI is investigated under the action of varying vertical loads and cyclic horizontal displacements by FE analysis and then the influence of the vertical load on horizontal behaviour of the isolator is evaluated. In this study, the isolator is subjected simultaneously to four levels of the vertical load (350, 500, 650 and 800 kN) and three levels of horizontal displacement amplitude (80, 112.5 and 135 mm). The value 350 kN of vertical load is a design vertical load for the isolator. The magnitude of design vertical load corresponds to axial force of column and the value is obtained from the analysis of the actual building. Besides, the horizontal behaviour of the prototype U-FREI is investigated under the design vertical load (350 kN) and cyclic horizontal displacement up to 80 mm by experimental study /11, 20/. Thus, the value 80 mm of horizontal displacement amplitude is selected to evaluate the accuracy of the FE model. The investigation process from FE analysis is conducted as follows.

Firstly, the isolator is loaded simultaneously to the design vertical load of 350 kN and two complete sinusoidal cycles of horizontal displacement of amplitude 80 mm ($0.89t_r$), as shown in Fig. 3, applied at the top rigid plate. Next, the vertical load is increased to three levels of 500, 650 and 800 kN. For the amplitude of cyclic horizontal displacement and each vertical load, the hysteresis loops of the isolator represent the relationship between shear forces and cyclic horizontal displacements are determined from FE analysis results and then its mechanical properties including effective horizontal stiffness and equivalent viscous damping factor are obtained.

The amplitude of cyclic horizontal displacement is subsequently increased (112.5 and 135 mm) and the process is repeated considering the same values for the vertical load as above. The complete simulation is considered for four vertical loads of P = 350, 500, 650, 800 kN and three displacement amplitudes of u = 80, 112.5 and 135 mm ($0.89t_r$, $1.25t_r$ and $1.50t_r$, respectively), a total of 12 FE simulation.

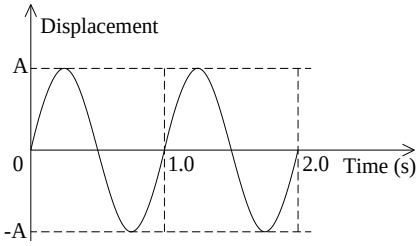

Figure 3. Imposed horizontal displacement history.

FE solution

The full transient dynamic analysis is carried out to determine the time-varying responses of the isolator. The full method uses the full system matrices to calculate transient responses. It is the most general method of analysis used in ANSYS. This method allows calculation of all types of nonlinearities, loads, displacements and stresses in a single pass and there are no mass matrix approximations involved. Full method is used in analysing the isolators because of the material nonlinearity and nonlinearity of the contact element. Displacement-based convergence criterion is used for the analysis under combined action of vertical load and horizontal displacements.

Effect of mesh size on FE analysis result

The model is meshed with hexagonal volume sweep. The volume sweep fills existing unmeshed volume with elements by sweeping the mesh from an adjacent area through the volume. If the area is not already meshed, volume sweep meshes the area and then extrudes it. In case of nonlinear and large displacement FE analysis, size of mesh plays an important role. Generally, a refined mesh gives more accurate solution in FE analysis. However, very fine mesh obviously requires large storage space as well as more computational time. Thus, a mesh sensitivity analysis is first carried out to arrive at an acceptable refined mesh by studying the solution convergence with mesh refinement, which is subsequently considered for the detailed analysis.

Figure 4 shows three FE models of the U-FREI with different discretization named as coarse, fine and very fine mesh size. The *x*-axis matches with fibers oriented along 0°, while *y*-axis matches with fibers along 90°. The U-FREI is investigated under the design verical load of 350 kN and horizontal displacement amplitude of 135 mm by FE analysis. Distribution of normalized stress S_{33}/p (p is the vertical pressure due to applied vertical load at the top of isolator, axis-3 is parallel to *z*-axis) plotted along the width of the 9th elastomer layer located adjacent to the mid-height and of the 9th fiber layer located at mid-height of the U-FREI at horizontal displacement of 135 mm are shown in Figs. 5 and 6, respectively. All the three types of FE meshes as shown in Fig. 4 are considered for the study. It can be seen from Fig. 5 that the stress distribution pattern, peak values of compressive stress in the mid elastomer layer corresponding to the coarse and fine mesh are very close to results obtained from very fine mesh. However, it may be observed from Fig. 6 that the stress distribution corresponding to very fine mesh is much smoother as compared to other two mesh cases, though the peak compressive values are almost in the same range. In view of this, all the subsequent analyses for all the considered isolators are carried out utilizing the very fine mesh as shown in Fig. 4c.

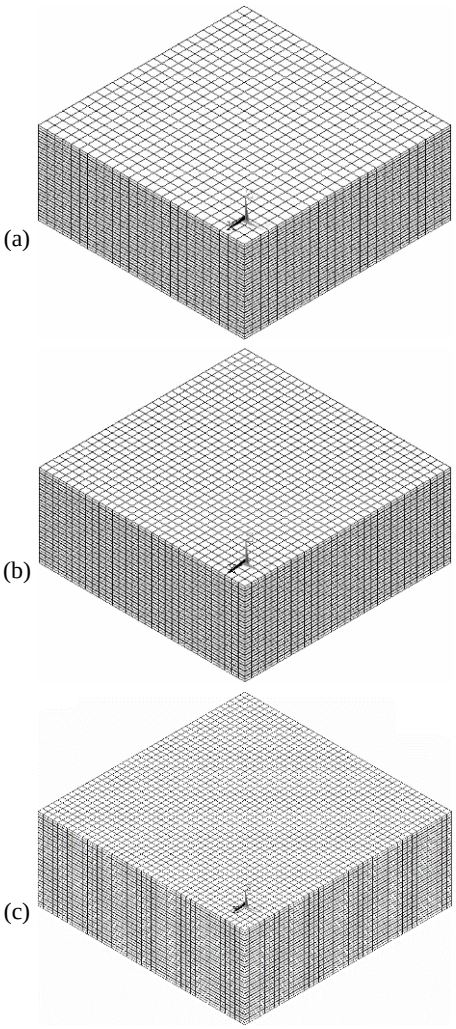

Figure 4. FE model of the U-FREI with different discretization: a) coarse mesh; b) fine mesh; c) very fine mesh.

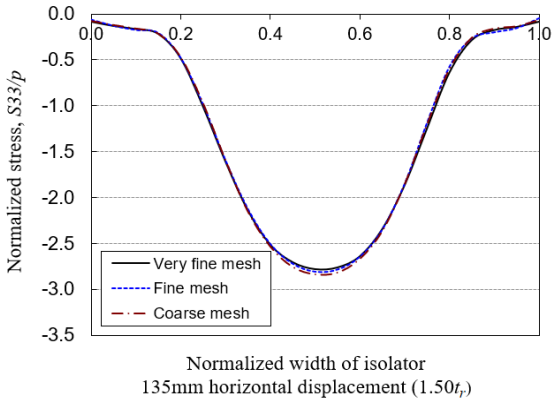

Figure 5. Distribution of normalized stress S_{33}/p plotted along the width in the elastomer layer at mid-height of U-FREI at displacement of 135 mm.

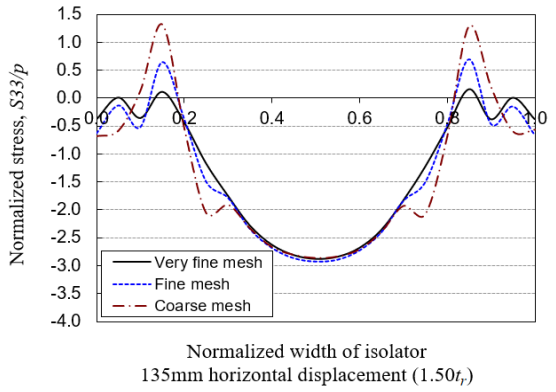

Figure 6. Distribution of normalized stress S_{33}/p plotted along the width in the fiber layer at mid-height of the U-FREI at displacement of 135 mm.

Validation of FE model of the U-FREI

According to /20/, the experimental study of the U-FREI under the design vertical load of 350 kN and cyclic horizontal displacement up to 80 mm was investigated at Structural Engineering Laboratory, Indian Institute of Technology Guwahati, India. Comparison of the horizontal response of the U-FREI from experimental and FE analysis results is conducted to evaluate the accuracy of the FE model.

Deformed shapes of the U-FREI as obtained from both FE analysis and experimental results at the horizontal displacement amplitude of 80 mm are shown in Fig. 7. The top and bottom surfaces of U-FREI exhibit stable roll off the contact surfaces without any damage. It can be seen from Fig. 7 that the deformed shape of the isolator obtained from FE analysis is in very good agreement with the deformed shape during the experimental test.

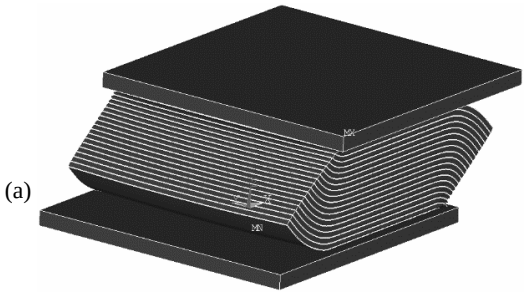

(b)

Figure 7. Deformed shapes of U-FREI at displacement amplitude of 80 mm and vertical force equal to 350 kN: a) FE analysis result; b) experimental result.

Hysteresis loops of an isolator represent the relationship between shear forces and cyclic horizontal displacements. For FE analysis results, the total forces in the loading direction at all nodes of the top surface of the isolator are summed to get the total shear force. Shear forces are then plotted against the horizontal displacement to get the hysteresis loops of the isolator. Comparison of the hysteresis loops of the U-FREI with increasing horizontal displacement up to 80 mm as obtained from experimental and FE analysis results is presented in Fig. 8, which shows a very good agreement between the expriment and FE analysis.

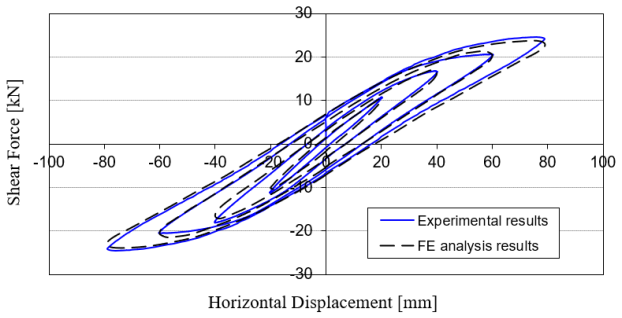

Figure 8. Comparison of hysteropesis loops of the U-FREI obtained from experiment and FE analysis.

Based on this observation, the accuracy of the adopted FE model is established. In view of this, the FE model is considered for the analysis of the cyclic response of the U-FREI up to higher displacement amplitudes (from 80 to 135 mm), wherein analysis is done for varying vertical loads as well as cyclic horizontal displacement.

EFFECT OF VERTICAL LOAD ON PERFORMANCE OF PROTOTYPE U-FREI

Hysteresis loops and backbone curves

The nonlinear behaviour of an isolator is generally reflected in its horizontal force-displacement hysteresis loop. Figures 9, 10 and 11 show hysteresis loops of the U-FREI under different vertical loads and horizontal displacement amplitude of 80, 112.5, and 135 mm, respectively.

The shapes of hysteresis loops of the prototype U-FREI under different vertical loads and cyclic horizontal displacement as obtained from FE analysis in this study are similar to those in the observation made by De Raaf et al. /18/ based on the experimental results of a scaled model of U-FREI. Thus, the adopted FE analysis model is very effective in evaluating the dynamic response of the prototype U-FREI under the variation of vertical load and cyclic horizontal displacement.

(a)

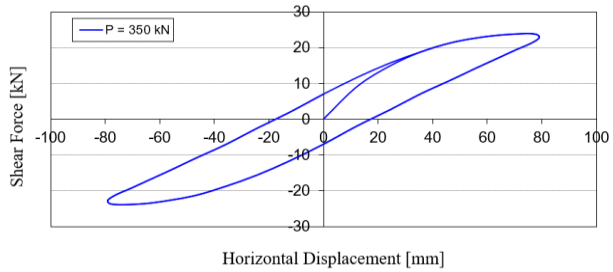

(b)

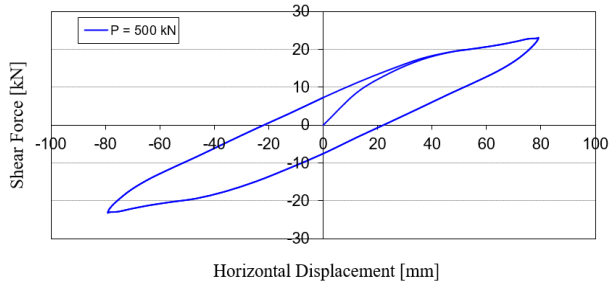

(c)

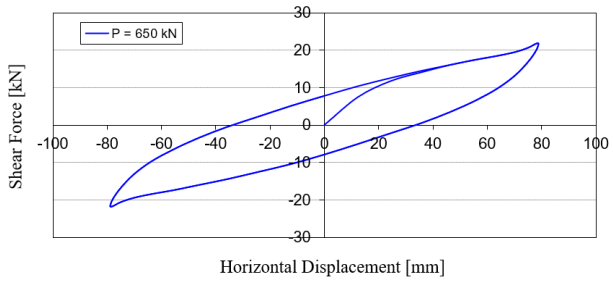

(d)

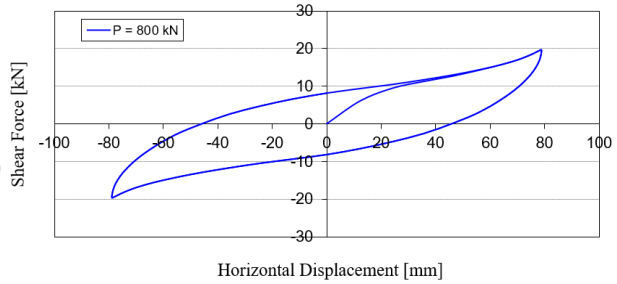

Figure 9. Hysteresis loops of the U-FREI under different vertical loads and horizontal displacement amplitude of 80 mm: a) P = 350 kN; b) P = 500 kN; c) P = 650 kN; d) P = 800 kN.

(a)

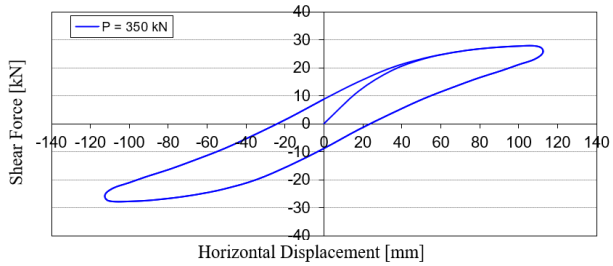

(b)

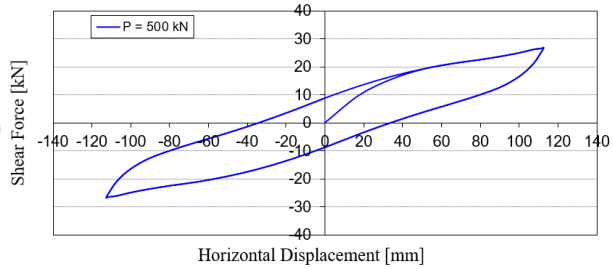

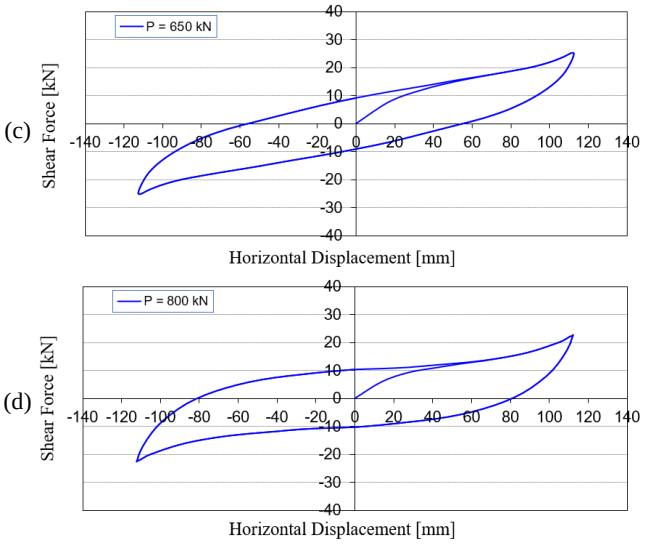

Figure 10. Hysteresis loops of U-FREI under different vertical loads and horizontal displacement amplitude of 112.5 mm: a) P = 350 kN; b) P = 500 kN; c) P = 650 kN; d) P = 800 kN.

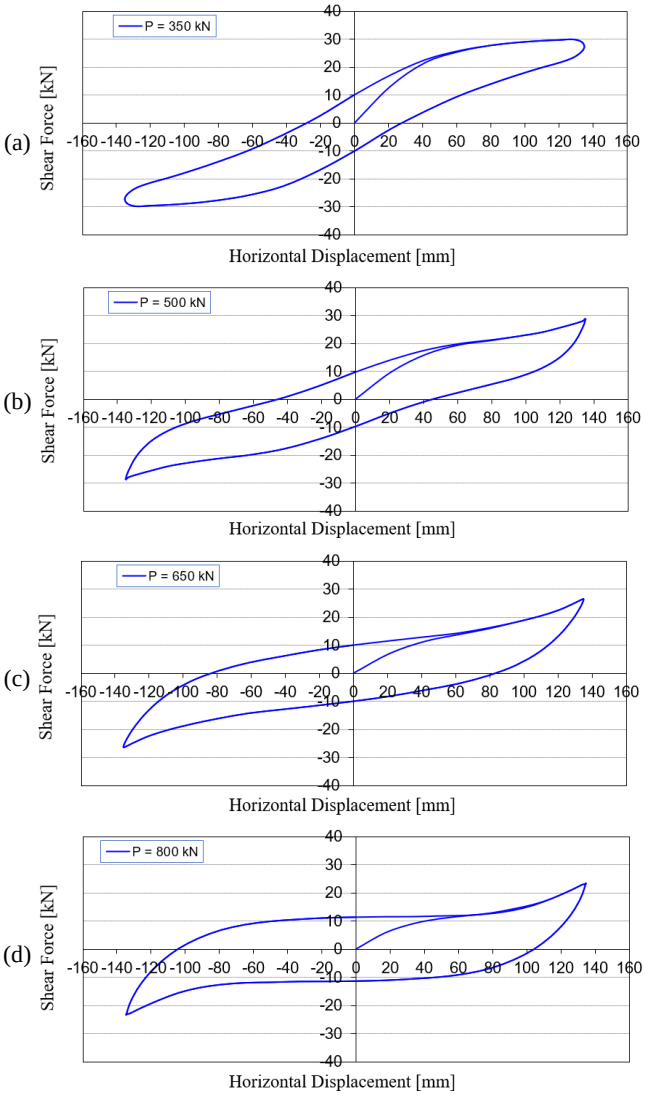

Figure 11. Hysteresis loops of the U-FREI under different vertical loads and horizontal displacement amplitude of 135mm: a) P = 350 kN; b) P = 500 kN; c) P = 650 kN; d) P = 800 kN.

In order to evaluate the influence of the vertical load on the horizontal behaviour of the U-FREI, a curve is fitted to shear force-displacement hysteresis loop. The fitted curve, denoted as backbone curve, represents an idealized evaluate of horizontal response of the isolator with the damping forces removed. The damping of an isolator is computed by measuring the energy dissipated in each cycle which is the area enclosed by the hysteresis loop. It is presented in more details in the next section. The fitted backbone curve is obtained from the average value of shear forces at any given horizontal displacement in the corresponding hysteresis loop as shown in Fig. 12.

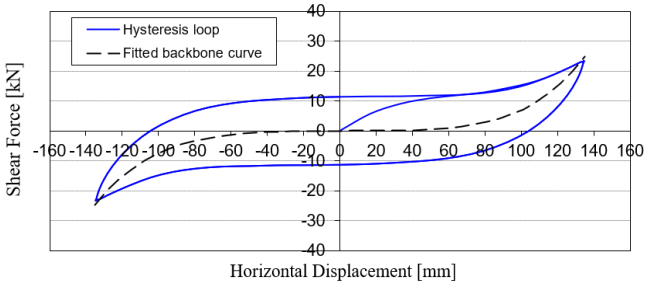

Figure 12. Illustration of a fitted backbone curve in a hysteresis loop of the U-FREI under vertical load of 800 kN and horizontal displacement amplitude of 135 mm.

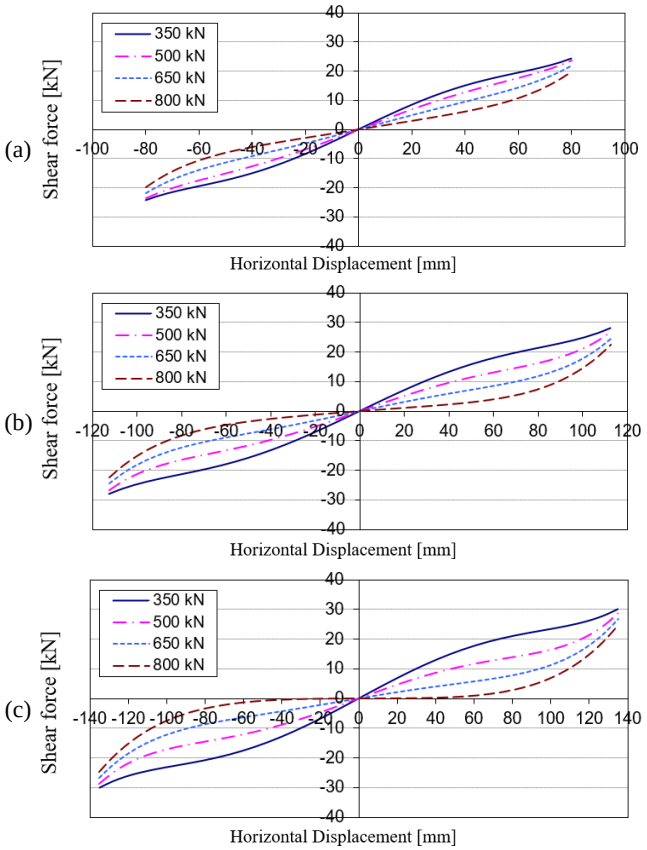

Figure 13. Backbone curves of U-FREI under variation of vertical loads and horizontal displacement amplitudes: a) u = 80 mm; b) u = 112.5 mm; c) u = 135 mm.

The backbone curves of U-FREI under different vertical loads (350, 500, 650 and 800 kN) and displacement amplitudes are shown in Fig. 13. It can be seen from Fig. 13 that the shear force of U-FREI decreases with the increase in

vertical load at each amplitude of horizontal displacement. It will result in a decrease in the effective horizontal stiffness of the isolator.

Mechanical properties of the U-FREI

Two important parameters such as effective horizontal stiffness and equivalent viscous damping factor (or damping factor) are obtained from the hysteresis loops. According to /25/, the effective horizontal stiffness of an isolator at any amplitude of horizontal displacement is defined as:

$$K_{eff}^{h} = \frac{F_{\max} - F_{\min}}{u_{\max} - u_{\min}}, \quad (6)$$

where: F_{max}, F_{min} are maximum and minimum values of the shear force; u_{max}, u_{min} are maximum and minimum values of the horizontal displacement.

The equivalent viscous damping factor of the isolator (β) is computed by measuring the energy dissipated in each cycle (W_d), which is the area enclosed by the hysteresis loop. The magnitude of β is computed as:

$$\beta = \frac{W_d}{2\pi K_{eff}^{h} \Delta_{\max}^{2}}, \quad (7)$$

where: Δ_{max} is the average of positive and negative maximum displacements, $\Delta_{max} = (|u_{max}| + |u_{min}|)/2$.

Effective horizontal stiffness and equivalent viscous damping factor of the isolator under different vertical loads and horizontal displacement amplitudes are presented in Table 1. These results are obtained by considering average values over two cycles of each horizontal displacement amplitude. The influence of vertical load on the mechanical properties, including effective horizontal stiffness and equivalent viscous damping factor, of the isolator under cyclic horizontal displacement is plotted in Figs. 14 and 15.

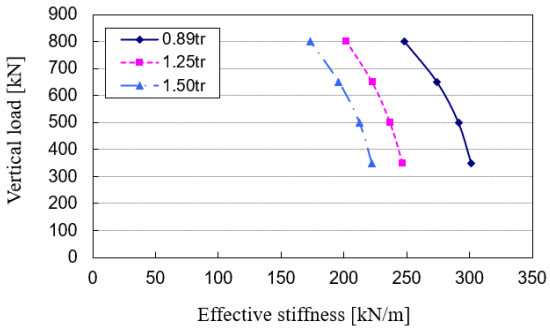

Figure 14. Effective horizontal stiffness of the U-FREI vs. vertical load for various horizontal displacement amplitudes.

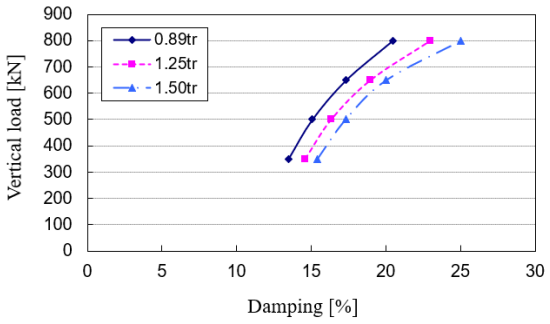

Figure 15. Equivalent viscous damping factor of the U-FREI vs. vertical load for various horizontal displacement amplitudes.

Table 1. Mechanical properties of the U-FREI under different vertical loads.

Vertical load P (kN)	Amplitude of horizontal displacement, u					
	80 mm		112.5 mm		135 mm	
	K_{eff}^{h} (kN/m)	β (%)	K_{eff}^{h} (kN/m)	β (%)	K_{eff}^{h} (kN/m)	β (%)
350	301.67	13.46	247.09	14.58	222.03	15.42
500	291.52	15.07	237.04	16.32	212.30	17.31
650	274.37	17.35	222.73	18.95	195.92	20.02
800	248.34	20.49	202.13	22.96	173.26	25.00

It is apparent from Table 1, Figs. 14 and 15 that the effective horizontal stiffness of the U-FREI decreases, while the equivalent viscous damping factor increases with the increase in the vertical load at any given amplitude of horizontal displacement. The decreases in effective stiffness are found to be 17.7%, 18.2% and 22.0% under vertical load ranging from 350 to 800 kN at the displacement amplitude of 80 mm ($0.89t_r$), 112.5 mm ($1.25t_r$), and 135 mm ($1.50t_r$), respectively. This finding is in agreement with the observation made by De Raaf et al. /18/ based on experimental results of a scaled model of U-FREI under different vertical loads. Moreover, for a given vertical load, the effective horizontal stiffness decreases, while the damping factor increases with increasing horizontal displacement amplitude. The decrease in effective stiffness corresponding to increase in amplitude of horizontal displacement from 80 to 135 mm are found to be 26.4%, 27.2%, 28.6% and 30.2% at vertical load of 350, 500, 650 and 800 kN, respectively. These reductions are due to rollover deformation, which results in an increase in the time period of the base isolated structure leading to increase in their seismic response control efficiency. Despite the reduction in the effective horizontal stiffness at high vertical loads, the U-FREI can maintain symmetric force-displacement hysteresis loops under cyclic loading.

In the above, it has been proven that the vertical load has a large influence on the horizontal response of an U-FREI. In engineering practice the isolator is generally considered to be subjected to a constant design vertical load and cyclic horizontal displacement during the design process of a base isolated building. However, the actual value of the vertical load applied (factored column load) may change for various reasons (e.g. due to the presence of live loads on a building or traffic volume on a bridge structure). To control the behaviour of U-FREIs supporting a base isolated building, it is thus necessary to consider the load combinations that lead to different axial loads of a column during the design process of the U-FREIs.

CONCLUSIONS

In this study, the influence of vertical loads on the performance of a prototype U-FREI is presented by FE analysis. The prototype isolator from which experimental results are obtained has been installed in an actual building in Tawang, India. Its size is 250×250×100 mm and its shape factor is 12.5. The U-FREI is subjected to various levels of vertical loads under cyclic horizontal displacement to determine the effect of vertical load on its dynamic properties. The concluding remarks are as follows:

- Generally, the effective horizontal stiffness of the U-FREI decreases due to rollover deformation, while the equivalent viscous damping factor increases with increasing amplitude of the horizontal displacement at a given value of applied vertical load.
- Effective horizontal stiffness of the U-FREI decreases, while the damping factor increases with the increase in the vertical load at any given amplitude of horizontal displacement.
- To control the behaviour of U-FREIs supporting a base isolated building, it is necessary to consider the load combinations that lead to different axial loads of a column during the design process of the U-FREIs.

REFERENCES

1. Vasiliadis, L.K. (2016), *Seismic evaluation and retrofitting of reinforced concrete buildings with base isolation systems*, Earthquakes and Struct. 10(2): 293-311. doi: 10.12989/eas.2016.10.2.293
2. Luo, J., Fahnestock, L.A., LaFave, J.M. (2017), *Nonlinear static pushover and eigenvalue modal analyses of quasi-isolated highway bridges with seat-type abutments*, Structures, 12: 145-167. doi: 10.1016/j.istruc.2017.08.006
3. Kumar, P., Petwal, S. (2019), *Seismic performance of secondary systems housed in isolated and non-isolated building*, Earthquakes and Struct. 16(4): 401-413. doi: 10.12989/eas.2019.16.4.401
4. Kelly, J.M. (1999), *Analysis of fibre-reinforced elastomeric isolators*, J Seismol. Earthquake Eng. 2(1): 19-34.
5. Moon, B.Y., Kang, G.J., Kang, B.S., Kelly, J.M. (2002), *Design and manufacturing of fiber reinforced elastomeric isolation*, J Mater. Proc. Technol. 130-131: 145-150. doi: 10.1016/S0924-0136(02)00713-6
6. Toopchi-Nezhad, H., Tait, M.J., Drysdale, R.G. (2008), *Testing and modeling of square carbon fiber-reinforced elastomeric seismic isolators*, Struct. Control Health Monit. 15(6): 876-900. doi: 10.1002/stc.225
7. Toopchi-Nezhad, H., Tait, M.J., Drysdale, R.G. (2009), *Parametric study on the response of stable unbonded-fiber reinforced elastomeric isolator (SU-FREIs)*, J Compos. Mater. 43 (15): 1569-1587. doi: 10.1177/0021998308106322
8. Strauss, A., Apostolidi, E., Zimmermann, T., et al. (2014), *Experimental investigations of fiber and steel reinforced elastomeric bearings: Shear modulus and damping coefficient*, Eng. Struct. 75(15): 402-413. doi: 10.1016/j.engstruct.2014.06.008
9. Van Engelen, N.C., Osgooei, P.M., Tait, M.J., Konstantinidis, D. (2014), *Experimental and finite element study on the compression properties of Modified Rectangular Fiber-Reinforced Elastomeric Isolators (MR-FREIs)*, Eng. Struct. 74(1): 52-64. doi: 10.1016/j.engstruct.2014.04.046
10. Das, A., Dutta, A., Deb, S.K. (2015), *Performance of fiber-reinforced elastomeric base isolators under cyclic excitation*, Struct. Cont. Health Monit. 22(2): 197-220, doi: 10.1002/stc.1668
11. Ngo, V.T., Dutta, A., Deb, S.K. (2017), *Evaluation of horizontal stiffness of fibre-reinforced elastomeric isolators*, Earthquake Eng. Struct. Dyn. 46(11): 1747-1767. doi: 10.1002/eqe.2879
12. Ngo, V.T., Deb, S.K., Dutta, A. (2018), *Effect of horizontal loading direction on performance of prototype square unbonded fibre reinforced elastomeric isolator*, Struct. Cont. Health Monit. 25(3). doi: 10.1002/stc.2112
13. Losanno, D., Spizzuoco, M., Calabrese, A. (2019), *Bidirectional shaking-table tests of unbonded recycled-rubber fiber-reinforced bearings (RR-FRBs)*, Struct. Cont. Health Monit. 26(9). doi: 10.1002/stc.2386
14. Calabrese, A., Losanno, D., Spizzuoco, M., et al. (2019), *Recycled rubber fiber-reinforced bearings (RR-FRBs) as base isolators for residential buildings in developing countries: The demonstration building of Pasir Badak, Indonesia*, Eng. Struct. 192: 126-144. doi: 10.1016/j.en gstruct.2019.04.076
15. Koh, C.G., Kelly, J.M. (1989), *Viscoelastic stability model for elastomeric isolation bearings*, J Struct. Eng. 115(2): 285-302. doi: 10.1061/(ASCE)0733-9445(1989)115:2(285)
16. Buckle, I.G., Liu, H. (1994), *Experimental determination of critical loads of elastomeric isolators at high shear strain*, NCEER Bulletin, 8(3): 1-5.
17. Nagarajaiah, S., Ferrell, K. (1999), *Stability of elastomeric seismic isolation bearings*, J Struct. Eng. 125(9): 946-954. doi: 10.1061/(ASCE)0733-9445(1999)125:9(946)
18. De Raaf, M.G.P., Tait, M.J., Toopchi-Nezhad, H. (2011), *Stability of fibre-reinforced bearings in an un-bonded application*, J Compos. Mater. 45(18): 1873-1884. doi: 10.1177/0021998310388319
19. Naeim, F., Kelly, J.M., Design of Seismic Isolated Structures: From Theory to Practice, John Wiley & Sons, New York, USA, 1999.
20. Ngo, V.T. (2020), *Effect of shape factor on the horizontal response of prototype unbonded fiber reinforced elastomeric isolators under cyclic loading*, Struct. Integ. and Life, 20(3): 303-312.
21. ANSYS version 14.0, Help System, Analysis Guide, ANSYS, Inc, USA, 2014
22. Ogden, R.W. (1972), *Large deformation isotropic elasticity - on the correlation of theory and experiment for incompressible rubber-like solids*, Proc. of the Royal Society A, 326(1567): 565-584. doi: 10.1098/rspa.1972.0026
23. Holzapfel, G.A. (1996), *On large strain viscoelasticity: Continuum formulation and finite element applications to elastomeric structures*, Int. J Numer. Methods Eng. 39(22): 3903-3926. doi: 10.1002/(SICI)1097-0207(19961130)39:22<3903::AID-NME3 4>3.0.CO;2-C
24. Wunderlich B., Thermal Analysis of Polymeric Materials, Handbook of Chemistry, Chichester: Springer, 2005.
25. ASCE/SEI 7-10, Minimum Design Loads for Buildings and Other Structures, American Society of Civil Engineers, Reston, Virginia, USA, 2013. doi: 10.1061/9780784412916